



Cite this: DOI: 10.1039/c7ce00808b

A series of transition metal coordination polymers based on a rigid bi-functional carboxylate–triazolate tecton†

 Nan-nan Mao,^{‡a} Peng Hu,^{‡a} Fan Yu,^b Xi Chen,^a Gui-lin Zhuang,^{id*} Tian-le Zhang,^{id*} and Bao Li^{id*}

By utilizing the pre-designed bi-functional ligand 4-(bis(4-benzoic)amino)-4*H*-1,2,4-triazole (H₂L), five new transition-metal-based coordination polymers, namely, {[Zn(L)]·H₂O·DMA}_n (1), {[Zn₂(L)₂]·DMF}_n (2), {[Mn(L)]·DMF}_n (3), {[Cd(L)]·DMA}_n (4) and [Cu₃(OH)₂(L)₂]_n (5) have been constructed and structurally characterized. In **1**, the tetrahedral zinc ion was incorporated in the final structure. However, complexes **2**, **3** and **4** bear 1D Zn-, Mn- and Cd-chains composed of metal ions, triazole and carboxyl groups, respectively. Differently, 1D [Cu₄(μ₃-OH)₂] chains had been stabilized in the 3D structure of **5**. In addition, the luminescence or magnetic properties of **1–5** had been correspondingly investigated with the consideration of their crystal structure. The whole research results manifest that utilizing a bi-functional ligand containing carboxyl and triazole groups is an efficient building method in constructing functional CPs.

 Received 27th April 2017,
Accepted 6th July 2017

DOI: 10.1039/c7ce00808b

rsc.li/crystengcomm

Introduction

The past two decades have witnessed the booming development of functional coordination polymers (CPs), because of their potential applications in the fields of gas sorption and separation, ion-exchange, catalysis, drug delivery, photo-luminescence, magnetism, *etc.*¹ The self-assembly of CPs depends on the coordination habit of the metal center, the structural character of the ligand, as well as other factors that influence the synthesis process such as temperature, pH value of the solution, and the solvent system.² A large part of attention paid to CPs has been done to understand the structure–activity relationship, which will be propitious to the development of structure design and oriented synthesis of the desired CPs.³ However, it is still a great challenge to synthesize CPs with predictable structures and desired properties.⁴ With the consideration of the synthesis conditions, tactical synthesis or se-

lection of the organic ligand and control of the reaction conditions are key factors for achieving expected CPs. Among the numerous ligands employed in CPs, versatile polycarboxylate ligands that could assume different kinds of bridging or chelating modes have been extensively employed in the preparation of CPs with novel structural motifs and interesting properties.⁵ In comparison, CPs with N-containing ligands have to some extent gained less interest. The syntheses of new N-donor ligands are a long-standing fascination of chemists, and so far, many bi-, tri-, and multidentate N-donor ligands with or without a N-heterocyclic backbone have been reported.⁶ The 1,2,4-triazole ligand and its derivatives presenting a hybrid of pyrazole and imidazole have been demonstrated to be effective in the construction of functional CP materials by virtue of their potential bridging patterns. The triazole group could exhibit versatile coordination modes, and results in variable functional materials based on the appropriate connection modes and metal ions.⁷ With the consideration of the superiority of aromatic carboxyl and triazole ligands, the utilization of a ligand that fuses two functional groups into one linker as a candidate in the fabrication of intriguing structures in the self-assembly process of CPs is promising.⁸

Herein, a rigid ligand possessing two carboxylic groups in symmetrical positions and a N-donor triazole group, namely, 4-(bis(4-benzoic)amino)-4*H*-1,2,4-triazole (H₂L), was designed and synthesized.⁹ Different from other ligands possessing three functional groups in one, for the designed ligand H₂L, the binding directions of two carboxyl groups and the triazole group should lie in two orthogonal planes, which naturally

^a Key Laboratory of Material Chemistry for Energy Conversion and Storage, School of Chemistry and Chemical Engineering, Huazhong University of Science and Technology, Wuhan, Hubei, 430074, PR China. E-mail: libao@hust.edu.cn

^b Key Laboratory of Optoelectronic Chemical Materials and Devices of Ministry of Education, School of Chemical and Environmental Engineering, Jiangnan University, Wuhan, Hubei, 430056, PR China

^c Institute of Industrial Catalysis, College of Chemical Engineering, Zhejiang University of Technology, Zhejiang, 310023, PR China. E-mail: glzhuang@zjut.edu.cn

† Electronic supplementary information (ESI) available: Additional computational data (PDF), X-ray crystallographic data for **1** and **2** (CIF). CCDC 1542184–1542188. For ESI and crystallographic data in CIF or other electronic format see DOI: 10.1039/c7ce00808b

‡ These authors contribute equally.

satisfies a prerequisite for generation of 3D CPs with different metal nodes under variable synthesis conditions. In this paper, five transition metal CPs, namely, $\{[\text{Zn}(\text{L})]\cdot\text{H}_2\text{O}\cdot\text{DMA}\}_n$ (1), $\{[\text{Zn}_2(\text{L})_2]\cdot\text{DMF}\}_n$ (2), $\{[\text{Mn}(\text{L})]\cdot\text{DMF}\}_n$ (3), $\{[\text{Cd}(\text{L})]\cdot\text{DMA}\}_n$ (4) and $[\text{Cu}_3(\text{OH})_2(\text{L})_2]_n$ (5), have been prepared by the hydrothermal method by utilizing H_2L . In addition, the crystal structures, thermal stabilities, luminescence and magnetic properties of some of the complexes have been described in detail. Viewed from the final structures, the two nitrogen atoms of triazole could optionally coordinate one or two metal ions along with the change of synthesis conditions.

Experimental

Materials and general methods

The organic H_2L ligand (ref. 9) and other reagents for the syntheses were of analytical grade and used as received from commercial sources without further purification. Elemental analyses (C, H and N) were determined on a Perkin-Elmer 2400 analyzer. The IR spectra were recorded as KBr pellets on a Nicolet Avatar-360 spectrometer in the 4000–400 cm^{-1} region. Thermogravimetric analysis (TGA) was performed on a Perkin-Elmer TG-7 analyzer heated from 25 to 800 °C under air. The fluorescence spectra were measured on a FLS920 spectrophotometer. The magnetization and magnetic relaxation were measured by using a superconducting quantum interference device (SQUID) magnetometer from Quantum Design, Inc.

Synthesis of 4-{bis(4-benzoic)amino}-4H-1,2,4-triazole (H_2L)

The ligand synthesis route was patterned after ref. 10. Firstly, 4-amino-4H-1,2,4-triazole (3.36 g, 40 mmol) was added to a stirred suspension of potassium *tert*-butoxide (4.48 g, 40 mmol) in DMSO (30 mL) at 0 °C. After stirring at room temperature for 2 h, a solution of 4-fluorobenzonitrile (2.44 g, 20 mmol) in DMSO (10 mL) was added dropwise below 0 °C. The mixture was stirred for another 1.5 h at room temperature, then poured into water, and neutralized with 1 N HCl. The precipitate was filtered and recrystallized from water to afford the white solid, 4-((4-cyanophenyl)amino)-4H-1,2,4-triazole. $^1\text{H-NMR}$ (DMSO- d_6): δ : 6.57 (2H, d, $J = 9$ Hz), 7.69 (2H, d, $J = 9$ Hz), 8.83 (2H, s).

Secondly, 4-((4-cyanophenyl)amino)-4H-1,2,4-triazole (2.4 g, 0.013 mmol) was added to a suspension of sodium hydride (0.48 g) in *N,N*-dimethylformamide (DMF) (40 mL) with ice-cooling. The mixture was stirred for 30 min at 40–50 °C, and cooled to room temperature. 4-Fluorobenzonitrile (1.6 g, 0.026 mmol) was added and the reaction mixture was stirred for 2 h at 80 °C, then cooled to room temperature. Water was added to the resultant residue and the whole solution was extracted with CHCl_3 , the organic layer was washed with water, dried over Na_2SO_4 and then over vacuum. A yellow liquid was obtained. Water was added to the yellow liquid, the solution was stirred for 5 min, and 4-{bis(4-cyanophenyl)amino}-4H-1,2,4-triazole was obtained. $^1\text{H-NMR}$ (DMSO- d_6): δ : 7.04 (4H, d, $J = 9$ Hz), 7.69 (4H, d, $J = 9$ Hz) 8.44 (2H, s).

Thirdly, H_2O (10 ml) and EtOH (10 ml) were added to the above product, then the reaction mixture was stirred for 24 h at 100 °C, then cooled to room temperature and EtOH was removed from the solution. Then water (50 ml) was added and the resulting solution was filtered. Then 2M HCl was added dropwise until the pH = 3–4, and the precipitate was filtered and recrystallized from water to obtain the final product in 75% yield. IR (KBr, cm^{-1}): 3447, 3117, 1669, 1597, 1383, 1274, 1180, 1061, 774. $^1\text{H-NMR}$ (400 MHz, DMSO- d_6): δ : 12.96 (s, 2H), 9.23 (s, 2H), 7.97 (d, $J = 8.4$ Hz, 4H), 7.07 (d, $J = 8.8$ Hz, 4H). MP: 266.4–272.3 °C.

Synthesis of compound 1. A mixture of $\text{Zn}(\text{NO}_3)_2\cdot 6\text{H}_2\text{O}$ (16 mg, 0.054 mmol) and H_2L (9.1 mg, 0.028 mmol) was dissolved in 5 mL of DMA/EtOH/ H_2O (1 : 2 : 2, V/V/V). And the reaction mixture was sonicated for 5 minutes before heating at 85 °C in an isothermal oven for 3 days. A colorless crystal was obtained in 62% yield. IR (KBr, cm^{-1}): 3525, 3068, 1634, 1597, 1418, 1373, 1275, 1182, 1070, 783.

Synthesis of compound 2. A mixture of $\text{Zn}(\text{NO}_3)_2\cdot 6\text{H}_2\text{O}$ (15 mg, 0.05 mmol) and H_2L (8.1 mg, 0.025 mmol) was dissolved in 4 mL of DMF/ H_2O (1 : 3, V/V). And the reaction mixture was also sonicated for about 5 minutes before heating at 85 °C in an isothermal oven for 3 days. Then a colorless strip crystal was obtained in 49% yield. IR (KBr, cm^{-1}): 3546, 3068, 1671, 1596, 1417, 1383, 1273, 1178, 1075, 783.

Synthesis of compound 3. A mixture of $\text{MnCl}_2\cdot 4\text{H}_2\text{O}$ (10 mg, 0.05 mmol) and H_2L (8.1 mg, 0.025 mmol) was dissolved in 4 mL of DMF/ H_2O (1 : 3, V/V). And the reaction mixture was also sonicated for about 5 minutes before heating at 85 °C in an isothermal oven for 3 days. Then a colourless crystal was obtained in 60% yield. IR (KBr, cm^{-1}): 3437, 3088, 1662, 1597, 1409, 1305, 1265, 1169, 1061, 784.

Synthesis of compound 4. A mixture of H_2L (0.027 mol), $\text{Cd}(\text{NO}_3)_2\cdot 4\text{H}_2\text{O}$ (0.064 mmol) and HBF_4 (40% aqueous, 2 drops) in a DMA/EtOH/ H_2O mixed solvent (DMA 2 mL; EtOH 1 mL; H_2O 1 mL) was fully stirred at room temperature for 10 min, sealed in a 25 mL Teflon-lined autoclave and heated at 100 °C for 3 days. The autoclave was slowly cooled (5 °C h^{-1}) to ambient temperature. The resultant crystals were obtained in 55% yield. IR (KBr, cm^{-1}): 3439, 3096, 1615, 1548, 1394, 1305, 1263, 1182, 1060, 784.

Synthesis of compound 5. A mixture of H_2L (0.026 mmol) and $\text{Cu}(\text{NO}_3)_2\cdot 3\text{H}_2\text{O}$ (0.028 mmol) in a DMF/ $\text{CH}_3\text{CN}/\text{H}_2\text{O}$ mixed solvent (DMF 0.5 mL; CH_3CN 1.5 mL; H_2O 2 mL) was fully stirred at room temperature for 10 min, sealed in a 25 mL Teflon-lined autoclave and heated at 100 °C for 3 days. The autoclave was slowly cooled (5 °C h^{-1}) to ambient temperature. The resultant green crystals were obtained in 65% yield. IR (KBr, cm^{-1}): 3442, 3065, 1617, 1553, 1401, 1301, 1267, 1102, 1054, 778.

Single crystal X-ray diffraction

X-ray diffraction data of 1–2 were collected on an Oxford Gemini S Ultra diffractometer using Mo- $\text{K}\alpha$ ($\lambda = 0.71073$ Å) radiation at room temperature, while the crystal structures of

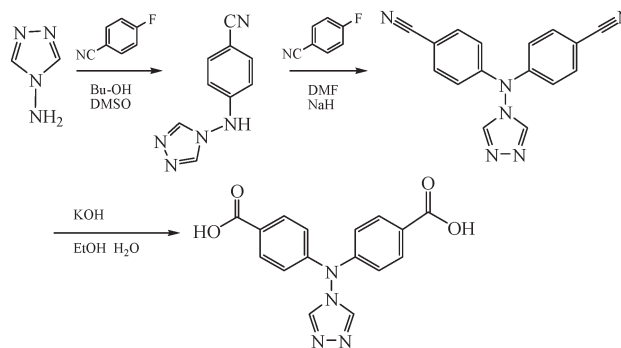
3–5 were obtained *via* BL17B at the Shanghai Synchrotron Radiation Facility (Shanghai, China) and processed with HKL3000.¹⁰ The structures of the complexes were solved by direct methods, and the non-hydrogen atoms were located from the trial structure and then refined anisotropically with SHELXTL using a full-matrix least squares procedure based on F^2 values.¹¹ The hydrogen atom positions were fixed geometrically at calculated distances and allowed to ride on the parent atoms. For 4, the weak diffraction intensity and corresponding restrictions must be responsible for the alert A. A summary of the structural determination and refinement for compound 1–5 is listed in Table 1.

Results and discussion

Synthesis of 1–5

The title ligand was synthesized according to the route in Scheme 1 summarized from the related references, and the crystalline samples were synthesized using a solvothermal method. The syntheses of compounds 1–5 were carried out with different metal salts and solvent systems. In the IR spectrum, the characteristic absorption peaks of the triazole group and other functional ones are clearly present. The strong absorption bands around 1586 and 1426 cm^{-1} are assigned to the triazole group peaks. The strong bands around 1600 and 1385 cm^{-1} are assignable to the asymmetric and symmetric stretching vibrations of the carboxylate groups. The absence of a band in the region of 1690–1730 cm^{-1} indicates complete deprotonation of the carboxylate groups and is consistent with the results of the X-ray diffraction analysis.

Crystal structure of 1. The single-crystal X-ray analysis reveals that 1 crystallizes in the orthorhombic *Pbca* space group, and the asymmetric unit consists of one crystallographically independent zinc atom and one L ligand (Fig. 1, up). The Zn atom is four-coordinated by three oxygen atoms and one nitrogen atom, which belong to the different li-



Scheme 1 The synthesis route of the ligand H_2L .

gands. Two of the oxygen atoms come from the *syn-syn* carboxylates, and other one belongs to the monodentate carboxylate. The coordination environment of the zinc center could be seen as a highly distorted tetrahedral coordination geometry with the angles ranging from 94.23(3) to 135.53(4) $^\circ$. The Zn–O/N bond lengths fall in the range of 1.935(1) to 2.017(2) Å, in accordance with the typical values of the Zn(II) state. Each L ligand is bound to four crystallographically different zinc atoms utilizing its carboxylate and triazole groups, to form a 3D coordination network (Fig. 1, down). Two coordination types of carboxylates have been observed in one ligand, which is bound to three zinc ions. The last zinc ion is linked with one nitrogen atom of the triazole group. Omitting the triazole group, a 2D layer constructed from the zinc-carboxylate layers could be observed. Considering 4-connected zinc ions and L ligands as four-connected nodes, a uninodal 4-connected 3D cage network with the point (Schläfli) symbol $\{4-6^5\}$ is topologically presented. Calculated using the PLATON routine, the solvent accessible volume in the dehydrated structure of 1 is about 28.8%.

Crystal structure of 2. Compared to the structure of 1, the different crystal structure of 2 is caused by the slight change of reaction conditions. Single-crystal X-ray analysis reveals

Table 1 Crystal data of 1–5

	1	2	3	4	5
Formula	$\text{C}_{20}\text{H}_{21}\text{N}_5\text{O}_6\text{Zn}$	$\text{C}_{38}\text{H}_{34}\text{N}_{10}\text{O}_{10}\text{Zn}_2$	$\text{C}_{19}\text{H}_{17}\text{MnN}_5\text{O}_5$	$\text{C}_{19}\text{H}_{17}\text{CdN}_5\text{O}_5$	$\text{C}_{32}\text{H}_{22}\text{Cu}_3\text{N}_8\text{O}_{10}$
Formula mass	492.81	921.53	450.32	434.69	869.23
Crystal system	Orthorhombic	Monoclinic	Orthorhombic	Orthorhombic	Monoclinic
$a/\text{Å}$	8.2270(6)	22.5432(16)	7.4830(15)	7.5850(15)	23.508(5)
$b/\text{Å}$	21.5096(9)	7.6652(4)	14.109(3)	14.052(2)	5.9780(12)
$c/\text{Å}$	23.8825(11)	22.7737(11)	17.972(4)	18.237(4)	25.257(5)
$\beta/^\circ$	90	102.378(6)	90	90	99.95(3)
Volume/ Å^3	4226.2(4)	3843.8(4)	1897.4(7)	1943.8(5)	3496.1(13)
Space group	<i>Pbca</i>	$P2_1/n$	$P2_12_12_1$	$P2_12_12_1$	$I2/a$
Z	8	4	4	4	4
R_{int}	0.0186	0.0293	0.0737	0.0810	0.0620
CCDC no.	1542184	1542185	1542186	1542187	1542188
GOOF	1.056	1.159	1.074	1.095	1.058
Flack parameters	—	—	0.498(16)	0.48(2)	—
R_1 ($I > 2\sigma(I)$)	0.0350	0.0533	0.0453	0.0513	0.0360
$wR(F^2)$ ($I > 2\sigma(I)$)	0.0808	0.1164	0.1229	0.1470	0.1009
R_1 (all data)	0.0435	0.0688	0.0453	0.0516	0.0378
$wR(F^2)$ (all data)	0.0871	0.1297	0.1229	0.1487	0.1029

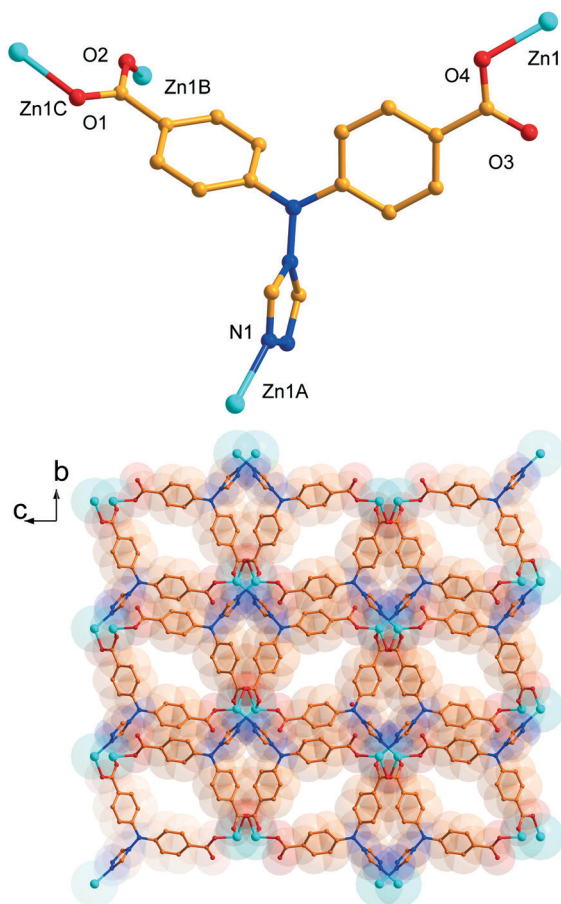


Fig. 1 The perspective view of an asymmetric unit (up) and the crystal packing mode (bottom) of **1**. Symmetric code: A, $x, -y + 3/2, z - 1/2$; B, $-x + 1, -y + 2, -z + 1$; C, $-x + 1/2, -y + 2, z - 1/2$.

that **2** crystallizes in the monoclinic $P2_1/n$ space group, and the asymmetric unit consists of two crystallographically different zinc atoms and two L ligands (Fig. 2a). The Zn1 atom is hexa-coordinated by four equatorial oxygen atoms from different *syn-syn* carboxylate groups of different ligands, and two nitrogen atoms belonging to the triazole groups of different ligands. The coordination environment of the zinc center could be seen as a highly distorted octahedral coordination geometry with the angles ranging from $82.93(2)$ to $110.87(3)^\circ$. In contrast, the Zn2 atom adopts a tetragonal pyramid configuration and coordinates to three oxygen atoms and two nitrogen atoms. The equatorial plane of the Zn2 atom is occupied by two oxygen atoms from two *syn-syn* carboxylate groups and two nitrogen atoms of triazole groups, while the axial site is occupied by one oxygen atom from a mono-dentate carboxylate group. The Zn–O/N bond lengths fall in the range of $1.988(3)$ to $2.172(4)$ Å, in accordance with the typical values of the Zn(II) state. Two types of 1D zinc chains have been observed in the packing structure. The adjacent Zn1 ions are inter-connected by two *syn-syn* carboxylates and one bridging triazole group of different ligands to form the 1D zinc chain, while the adjacent Zn2 ions are inter-linked *via* one *syn-syn* carboxylate and one bridging triazole group of different li-

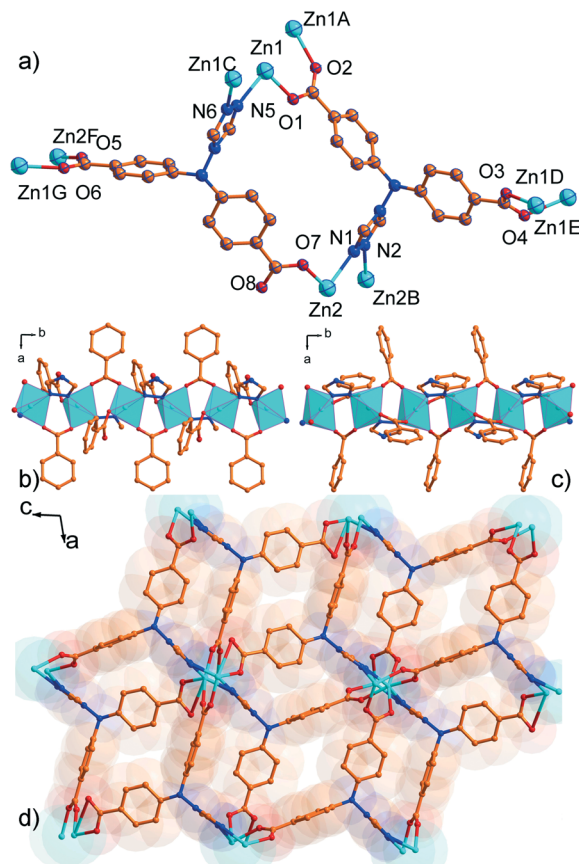


Fig. 2 The perspective view of the asymmetric unit (a), a 1D Zn(1) chain (b), a 1D Zn(2) chain (c) and the crystal packing mode (d) of **2**. Symmetric code: A, $-x + 1/2, y - 1/2, -z + 1/2$; B, $-x + 1/2, y - 1/2, -z + 3/2$; C, $-x + 1/2, -y + 1/2, -z + 1/2$; D, $-x + 1, -y + 1, -z + 1$; E, $1/2 + x, -y + 1/2, z + 1/2$; F, $-x, -y + 1, -z + 1$; G, $x - 1/2, -y + 3/2, z - 1/2$.

gands to form the other 1D zinc chain, as shown in Fig. 2b and c. In this way, two types of crystallographically different ligands coordinate six or five zinc ions to form the 3D coordination network (Fig. 2d). Calculated using the PLATON routine, the solvent accessible volume in the dehydrated structure of **2** is about 27.0%.

Crystal structure of 3. By substituting the zinc salt with a manganese one, a 3D Mn coordination polymer had been synthesized. Single-crystal X-ray analysis reveals that **3** crystallizes in the orthorhombic $P2_12_12_1$ space group, and the asymmetric unit consists of one manganese atom and one L ligand (Fig. 3a). The Mn1 atom is hexa-coordinated by four equatorial oxygen atoms from different *syn-syn* carboxylate groups of different ligands, and two nitrogen atoms belonging to the triazole groups of different ligands. The coordination environment of the Mn center could be seen as a slightly distorted octahedral coordination geometry with the angles ranging from $80.18(2)$ to $102.65(3)^\circ$. The Mn–O/N bond lengths fall in the range of $2.112(3)$ to $2.325(4)$ Å, in accordance with the typical values of the Mn(II) state. The adjacent Mn1 ions are inter-connected by two *syn-syn* carboxylates and one bridging triazole group of different ligands to form the 1D Mn chain, as shown in Fig. 3b. Each L ligand inter-

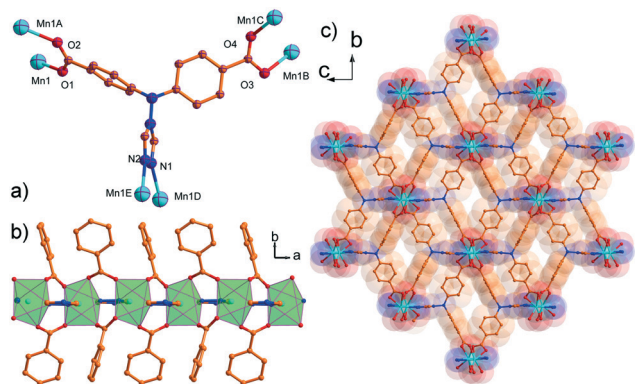


Fig. 3 The perspective view of an asymmetric unit (a), a 1D Mn(1) chain (b) and the crystal packing mode (c) of **3**. Symmetric code: A, $x + 1/2, -y + 1/2, -z + 1$; B, $x, y + 1, z$; C, $x - 1/2, -y + 3/2, -z + 1$; D, $-x + 1, y + 3/2, -z + 3/2$; E, $-x + 1/2, -y + 1, z + 1/2$.

connected six hexa-coordinated Mn ions to form the 3D coordination network (Fig. 3c). Calculated using the PLATON routine, the solvent accessible volume in the dehydrated structure of **3** is about 21.8%.

Crystal structure of 4. By reacting a cadmium ion with the bi-functional linker, a 3D Cd coordination polymer had been synthesized. Single-crystal X-ray analysis reveals that **4** exhibits a similar crystal structure to **3**, as expected from the different bridging mode between adjacent Cd ions. The coordination environment of the Cd center could be seen as a slightly distorted pentagonal bipyramid coordination geometry. The axial positions are occupied by two oxygen atoms of two *syn-syn* carboxylates, while the equatorial plane consisted of two nitrogen atoms of two triazole and three oxygen atoms of two $\mu_2\text{-}\eta^2\text{:}\eta^1$ carboxylate groups of two different ligands. The adjacent Cd1 ions are inter-connected by one *syn-syn* carboxylate, one bridging triazole group and one bridged oxygen atom of $\mu_2\text{-}\eta^2\text{:}\eta^1$ carboxylate of different ligands to form the 1D Cd chain, as shown in Fig. 4. Each L ligand interconnects six hepta-coordinated Cd ions to form the 3D coordination network. Calculated using the PLATON routine, the solvent accessible volume in the dehydrated structure of **4** is about 20.7%.

Crystal structure of 5. When the bi-functional ligand reacted with a copper ion, a different crystal structure (**5**) based on the connection of ligands and 1D $[\text{Cu}_4(\mu_3\text{-OH})_2]$

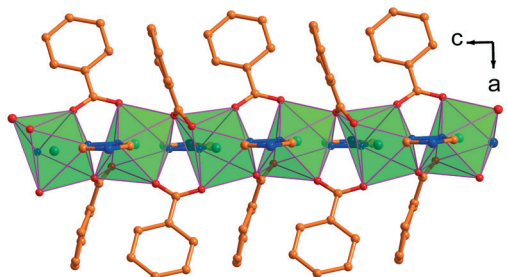


Fig. 4 The perspective view of a 1D Cd(1) chain of **4**.

chains had been synthesized. Single-crystal X-ray analysis reveals that **5** crystallizes in the monoclinic $C2/c$ space group, and the asymmetric unit consists of two crystallographically different copper atoms, one hydroxyl anion and one L ligand (Fig. 5a). The Cu1 atom is penta-coordinated with the geometric parameter τ of 0.487, indicating the particular case of a coordination environment between trigonal bipyramidal ($\tau = 1$) and rectangular pyramidal ($\tau = 0$).¹² The equatorial sites are occupied by two oxygen atoms from one mono-dentate carboxylate and one hydroxyl and one nitrogen atom of a bridging triazole group, while the axial sites are filled with two oxygen atoms from one *syn-syn* carboxylate group and one hydroxyl. In contrast, the coordination environment of the Cu2 center could be seen as a slightly distorted octahedral configuration. The equatorial plane consists of four oxygen atoms from two *syn-syn* carboxylate and two $\mu_3\text{-OH}$, while the axial positions are occupied by two nitrogen atoms from two bridging triazole. The Cu–O/N bond lengths fall in the range of 1.905(3) to 2.371(4) Å, in accordance with the typical values of the Cu(II) state. Two symmetric Cu1 ions are inter-connected by two $\mu_3\text{-OH}$, which means the sharing of one edge of two trigonal bipyramids. In addition, each $\mu_3\text{-OH}$

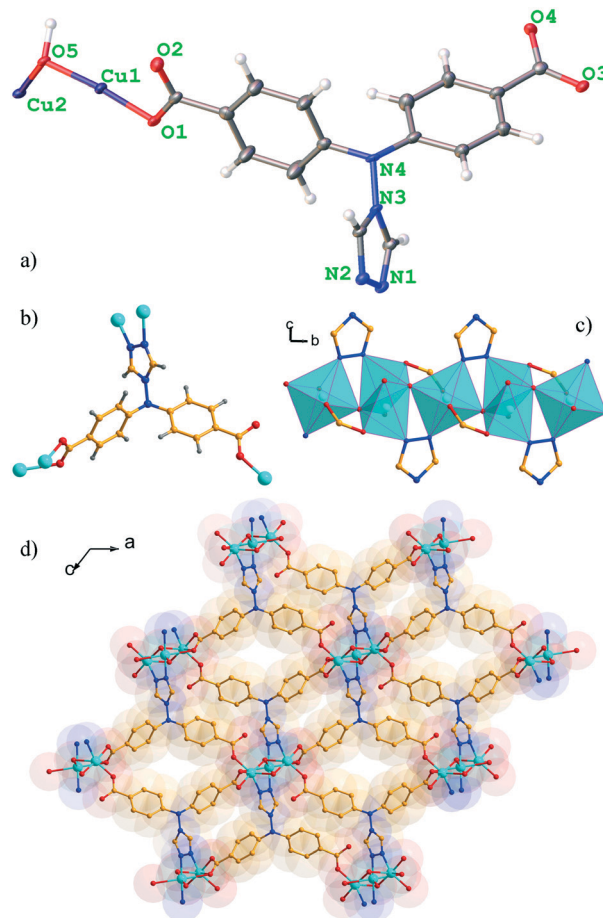


Fig. 5 The perspective view of an asymmetric unit (a), the connection mode of the ligand (b), a 1D $[\text{Cu}_4(\mu_3\text{-OH})_2]$ chain (c) and the crystal packing mode (d) of **5**.

still bonds one Cu²⁺ ion to form the 1D copper-hydroxyl chain, which is further stabilized by *syn-syn* carboxylate and bridging triazole groups, as shown in Fig. 5c. This copper-hydroxyl chain could be also seen as the duplication of [Cu₄(μ₃-OH)₂] by sharing the vertex of triangles to form the 1D chain structure. Each bi-functional linker bonds to five copper ions from three copper-hydroxyl chains to form the 3D crystal structure. Calculated using the PLATON routine, almost no solvent accessible volume in the dehydrated structure of 5 could be observed.

Comparison of different structures

By utilizing the newly designed bi-functional ligand containing carboxyl and triazole groups and reacting with different transitional metal ions, five 3D CPs had been constructed. In 1, the tetrahedral zinc ion was incorporated in the final structure. However, complexes 2, 3 and 4 bear a 1D chain composed of metal ions, triazole and carboxyl groups, respectively. Differently, 1D [Cu₄(μ₃-OH)₂] chains had been stabilized in 3D structure of 5. Comparing the connection modes of 1 and 2, the main difference might be ascribed to the coordination ability of the triazole group. When each triazole binds two zinc ions *via* two N atoms, a 1D metal chain could be achieved in the final structure. However, the triazole could also exhibit the monodentate coordination mode, which tends to result in a single-ion metal node in the final structure. The different reaction solvent systems must be responsible for the difference in the final structures.¹³ The solvent molecules were stabilized in the final structures *via* hydrogen bonding interactions, and the different steric effects of solvent molecules might disturb the coordination modes of triazole groups. For 1, the framework interacts with water molecules that have H-bonding interactions with DMA molecules; for 2, the guest DMF molecules have weak interactions with hydrogen atoms on triazole groups.¹⁴ For 2, 3, 4 and 5, similar 1D metal-chain structures could be observed except for the different coordination modes of carboxyl groups, which could be ascribed to the coordination habits of metal ions. Overall, as observed from all the final structures, the special bent configurations of the ligand and different weak interactions between the framework and solvent molecules must be responsible for the construction of versatile 3D CPs along with variable metal nodes.

Thermal stability analyses

To further estimate the thermal stability of these complexes, their thermal behaviors were investigated by thermogravimetric analyses (TGA) under a N₂ atmosphere (see Fig. S4†). For 1, the first weight loss occurred from 35 °C to 200 °C, indicating the release of the lattice DMA molecules. The weight loss was 20.2% (calc. 21.3%). The residual framework starts to decompose beyond 325 °C. For 2, a similar thermal behavior to 1 could be observed. The residual framework was stable up to 370 °C and then began to decompose. The highly-connected 1D zinc chain structure in 2 must

be responsible for the higher thermal stability than that of 1. The TGA curves of 3 and 4 are similar to 2, even though DMA molecules resided in the framework. For 5, it was stable up to 250 °C and then began to decompose. The existence of a [Cu₄(μ₃-OH)₂] unit and the absence of guest solvents must be responsible for the different thermal behavior compared to those of 1–4.

Luminescence properties of 1–3

The compounds constructed from d¹⁰ metal centers (such as Zn^{II} and Cd^{II} ions) and conjugated organic linkers could be potential candidates for photo-active materials. Therefore, the solid-state photo luminescence behaviors of 1, 2 and 4 as well as the free ligand were investigated in the solid state at room temperature. The spectrum shows that the free ligand displays an intense emission band at about 260 nm when excited at 378 nm which can be assigned to π* → n. Similar luminescence properties of 1–3 could be observed to free ligand, indicating the absence of efficient correlation of coordinated metal ions and deprotonated ligands.⁹

Magnetic properties of 4 and 5

The variable-temperature magnetic susceptibilities of 3 and 5 were measured using crystalline samples under 1 KOe in the range of 2–300 K and are shown as χ_MT and χ_M versus T plots in Fig. 6. For 3, χ_MT values at 300 K are about 4.35 emu K mol⁻¹, close to the experimental value of the spin-only value expected for one magnetically isolated Mn^{II} ion. Upon cooling, the χ_MT values gradually decrease and then quickly decline below 50 K, which are mainly ascribed to the total zero-field splitting of the Mn ion or possible intramolecular antiferromagnetic couplings. A similar magnetic behavior was observed for 5. The χ_MT values at 300 K are about 1.15 emu K mol⁻¹, lower than the experimental value of the spin-only value (1.125 emu K mol⁻¹ from g = 2.00) expected for three magnetically isolated Cu^{II} ions. The data above 150 K follow the Curie–Weiss law with C = 3.216 and 2.723 emu K mol⁻¹ and θ = -53.457 and -371.41 K. The above characteristics clearly suggest overall antiferromagnetic interactions between Mn^{II} or Cu^{II} ions in compounds 3 and 5.

Furthermore, magnetic fittings of M–T curves were performed for the studies of the magnetic coupling mechanism in 3 and 5. A glance of 3 and 5 can reveal that magnetic properties of 5 and 3 are governed by a one-dimensional Cu₄ unit-based chain and a one-dimensional single Mn-based chain, respectively. For 5, each Cu₄ unit contains three different magnetic propagation paths: μ₃-OH with ∠Cu–O–Cu = 118.77° and the N=N moiety of the ligand (J₁), two μ₃-OH bridges with ∠Cu–O–Cu = 96.37° (J₂), and a *syn-anti* carboxylate bridge (J₃), as shown in Fig. 6 (up: insert). For 3, each Mn(II) ion connects with adjacent ones by the bridge (J) of *syn-anti* carboxylate and the N=N moiety of the ligand. Thus, the Hamiltonian operator for 5 (eqn (1)) and 3 (eqn (2)) can be obtained as follows:

$$H = \sum_{i=1}^n [J_1(S_i S_{i+1} + S_{i+2} S_{i+3}) + J_2 S_{i+1} S_{i+2} + J_3(S_i S_{i+2} + S_{i+1} S_{i+3})] \quad (1)$$

$$H = -J \sum_{i=1}^n S_i S_{i+1} \quad (2)$$

A weak interaction (zJ) constant and single ion anisotropy (D) were considered for the description of **5** and **3**, respectively. Concerning the huge number of one-dimensional metal chains,¹⁵ the temperature-independent paramagnetism (TIP) parameter was also taken into account. In this fitting, we combined the high-efficiency searching performance of Genetic Algorithm and the high-precision of Quantum Monte Carlo method derived from the ALPS project¹⁶ (see the ESI†) to search the optimal parameters. According to the principle of the least reliability factor ($R = \sum[(\chi_M T)_{\text{obs}} - (\chi_M T)_{\text{calcd}}]^2 / \sum[(\chi_M T)_{\text{obs}}]^2$), we searched the globally best parameter toward the whole multi-dimensional space among 500 generations. And after searching for 500 generations (see Fig. S2†), the

obtained best parameters are presented as follows: $J_1 = -23.82 \text{ cm}^{-1}$, $J_2 = -180.03 \text{ cm}^{-1}$, $J_3 = 2.92 \text{ cm}^{-1}$, $g = 2.25$, $zJ = -0.60 \text{ cm}^{-1}$, $\text{TIP} = 6.8 \times 10^{-4} \text{ cm}^3 \text{ mol}^{-1}$, $R = 2.04 \times 10^4$ for **5**; $J = -0.35 \text{ cm}^{-1}$, $D = 2.07 \text{ cm}^{-1}$, $g = 1.71$, $\text{TIP} = 5.18 \times 10^{-4} \text{ cm}^3 \text{ mol}^{-1}$, $R = 6.44 \times 10^{-6}$ for **3**. For **5**, the conclusions are as follows: (1) J_1 of -23.82 cm^{-1} indicates antiferromagnetic exchange, contributed by a mixed bridge of $\mu_3\text{-OH}$ and the $\text{N}=\text{N}$ moiety of the ligand; (2) a larger J_2 of -180.03 cm^{-1} shows two $\mu_3\text{-OH}$ bridges induce a strong antiferromagnetic coupling, compatible with previous simulation results in a multinuclear cluster;¹⁷ (3) J_3 of 2.92 cm^{-1} uncovers the ferromagnetic exchanges in a *syn-anti* carboxylate bridge, associated with poor overlap of 3d magnetic orbitals.¹⁸ For **3**, a weak antiferromagnetic coupling of $J = -0.35 \text{ cm}^{-1}$ shows the synergic interaction of *syn-anti* carboxylate¹⁹ and the $\text{N}=\text{N}$ moiety of the ligand. And the D value of 2.07 cm^{-1} is good agreement with present results.²⁰

Conclusion

In summary, five new transition-metal-based CPs have been constructed from the designed bi-functional ligand 4-{bis(4-benzoic)amino}-4*H*-1,2,4-triazole, which exhibit diverse crystal structures based on different metal nodes. In **1**, the tetrahedral zinc ion was incorporated in the final structure. However, complexes **2**, **3** and **4** bear 1D chains comprised of metal ions, triazole and carboxyl groups, respectively. Differently, 1D $[\text{Cu}_4(\mu_3\text{-OH})_2]$ chains had been stabilized in 3D structure of **5**. In addition, the luminescence or magnetic properties of **1**–**5** had been correspondingly investigated with the consideration of their crystal structure. The whole research results manifest that utilizing a bi-functional ligand containing carboxyl and triazole groups is an efficient building method in constructing functional CPs. The bi-functional ligand could bring about not only the structural diversity of CPs, but also the variety of properties. These results will offer more insights into the intricate structure–functionality relationship of CPs and the rational design of new crystalline materials.

Acknowledgements

We gratefully acknowledge the National Natural Science Foundation of China (21471062) and the Open Project of the State Key Laboratory of Physical Chemistry of the Solid Surface (Xiamen University) (201616) for financial support and the Analytical and Testing Center, Huazhong University of Science and Technology, for analysis and spectral measurements. We also thank the staff from the BL17B beamline of the National Center for Protein Sciences Shanghai (NCPSS) at the Shanghai Synchrotron Radiation Facility for assistance during data collection.

Notes and references

- 1 Y. Bai, Y. Dou, L. Xie, W. Rutledge, J. Li and H. Zhou, *Chem. Soc. Rev.*, 2016, 45, 2327; J. Li, J. Sculley and H. Zhou, *Chem.*

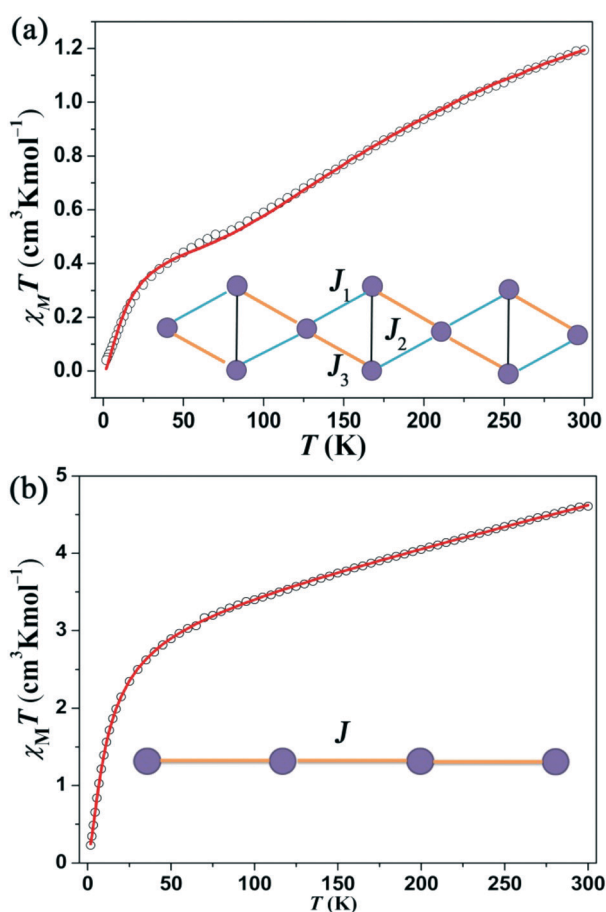


Fig. 6 Experiment plot of $\chi_M T$ vs. T (denoted \circ) and QMC fitting (red line) for **5** (a) and **3** (b) (inset figure is distribution sketch of $\text{Cu}(\text{II})$ or $\text{Mn}(\text{II})$ ions).

- Rev.*, 2012, **112**, 869; B. Wang, X. Lv, D. Feng, L. Xie, J. Zhang, M. Li, Y. Xie, J. Li and H. Zhou, *J. Am. Chem. Soc.*, 2016, **138**, 6204; J. Qin, D. Du, W. Guan, X. Bo, Y. Li, L. Guo, Z. Su, Y. Wang, Y. Lan and H. Zhou, *J. Am. Chem. Soc.*, 2015, **137**, 7169; J. Li, Y. Ma, M. C. McCarthy, J. Sculley, J. Yu, H. Jeong, P. B. Balbuena and H. Zhou, *Coord. Chem. Rev.*, 2011, **255**, 1791; J. Park, Q. Jiang, D. Feng, L. Mao and H. Zhou, *J. Am. Chem. Soc.*, 2016, **138**, 3518; A. Dhakshinamoorthy, A. M. Asiri and H. Garcia, *Angew. Chem., Int. Ed.*, 2016, **55**, 5414; P. Pachfule, M. K. Panda, S. Kandambeth, S. M. Shivaprasad, D. Diaz Diaz and R. Banerjee, *J. Mater. Chem. A*, 2014, **2**, 7944; C. Dey and R. Banerjee, *ChemPhysChem*, 2013, **14**, 1009.
- 2 Y. Cui, B. Li, H. He, W. Zhou, B. Chen and G. Qian, *Acc. Chem. Res.*, 2016, **49**, 483; R. R. Salunkhe, J. Tang, Y. Kamachi, T. Nakato, J. H. Kim and Y. Yamauchi, *ACS Nano*, 2015, **9**, 6288; L. Wang, X. Feng, L. Ren, Q. Piao, J. Zhong, Y. Wang, H. Li, Y. Chen and B. Wang, *J. Am. Chem. Soc.*, 2015, **137**, 4920; G. Lu, G. S. Li, Z. Guo, O. K. Farha, B. G. Hauser, X. Qi, Y. Wang, X. Wang, S. Han, X. Liu, J. S. DuChene, H. Zhang, Q. Zhang, X. Chen, J. Ma, S. C. J. Loo, W. D. Wei, Y. Yang, J. T. Hupp and F. Huo, *Nat. Chem.*, 2012, **4**, 310; Y. K. Deng, H. F. Su, J. H. Xu, W. G. Wang, M. Kurmoo, S. C. Lin, Y. Z. Tan, J. Jia, D. Sun and L. S. Zheng, *J. Am. Chem. Soc.*, 2016, **138**, 1328.
 - 3 H. Furukawa, K. E. Cordova, M. O'Keeffe and O. M. Yaghi, *Science*, 2013, **341**, 974; J. J. Low, A. I. Benin, P. Jakubczak, J. F. Abrahamian, S. A. Faheem and R. R. Willis, *J. Am. Chem. Soc.*, 2009, **131**, 15834; K. C. Stylianou, R. Heck, S. Y. Chong, J. Bacsá, J. T. A. Jones, Y. Z. Khimiyak, D. Bradshaw and M. J. Rosseinsky, *J. Am. Chem. Soc.*, 2010, **132**, 4119; M. M. Wanderley, C. Wang, C. Wu and W. Lin, *J. Am. Chem. Soc.*, 2012, **134**, 9050; C. Wang, J. Wang and W. Lin, *J. Am. Chem. Soc.*, 2012, **134**, 19895; M. Wriedt, A. A. Yakovenko, G. J. Haider, A. V. Prosvirin, K. R. Dunbar and H. Zhou, *J. Am. Chem. Soc.*, 2013, **135**, 4040; T. Kundu, S. C. Sahoo and R. Banerjee, *Chem. Commun.*, 2012, **48**, 4998.
 - 4 M. Zeng, Z. Yin, Y. Tan, W. Zhang, Y. He and M. Kurmoo, *J. Am. Chem. Soc.*, 2014, **136**, 4680; J. B. DeCoste, G. W. Peterson, B. J. Schindler, K. L. Killops, M. A. Browe and J. J. Mahle, *J. Mater. Chem. A*, 2013, **1**, 11922; R. Decadt, K. Van Hecke, D. Depla, K. Leus, D. Weinberger, I. Van Driessche, P. Van der Voort and R. Van Deun, *Inorg. Chem.*, 2012, **51**, 11623; C. Ren, L. Hou, B. Liu, G. Yang, Y. Wang and Q. Shi, *Dalton Trans.*, 2011, **40**, 793; F. Huang, Q. Zhang, Q. Yu, H. Bian, H. Liang, S. Yan, D. Liao and P. Cheng, *Cryst. Growth Des.*, 2012, **12**, 1890; Y. Wang, J. Fu, J. Wei, X. Xu, X. Li and Q. Liu, *Cryst. Growth Des.*, 2012, **12**, 4663; C. Ren, P. Liu, Y. Wang, W. Huang and Q. Shi, *Eur. J. Inorg. Chem.*, 2010, 5545; P. Pachfule, Y. Chen, S. C. Sahoo, J. Jiang and R. Banerjee, *Chem. Mater.*, 2011, **23**, 2908.
 - 5 G. Liu, X. Li and L. Wang, *CrystEngComm*, 2013, **15**, 2428; K. Zhang, N. Qiao, H. Gao, F. Zhou and M. Zhang, *Polyhedron*, 2007, **26**, 2461; Y. Ling, Z. Chen, H. Zheng, Y. Zhou, L. Weng and D. Zhao, *Cryst. Growth Des.*, 2011, **11**, 2811; L. Cheng, J. Wang and S. Gou, *Inorg. Chem. Commun.*, 2011, **14**, 261; D. S. Chowdhuri, A. Rana, M. Bera, E. Zangrando and S. Dalai, *Polyhedron*, 2009, **28**, 2131; A. D. Naik, M. M. Dirtu, A. Leonard, B. Tinant, J. Marchand-Brynaert, B. Su and Y. Garcia, *Cryst. Growth Des.*, 2010, **10**, 1798; D. Sarma, V. Srivastava and S. Natarajan, *Dalton Trans.*, 2012, **41**, 4135; B. Garai, A. Mallick and R. Banerjee, *Chem. Sci.*, 2016, **7**, 2195.
 - 6 Y. Li, W. Zou, M. Wu, J. Lin, F. Zheng, Z. Liu, S. Wang, G. Guo and J. Huang, *CrystEngComm*, 2011, **13**, 3868; J. Li, Y. Peng, H. Liang, Y. Yu, B. Xin, G. Li, Z. Shi and S. Feng, *Eur. J. Inorg. Chem.*, 2011, 2712; G. A. Senchyk, A. B. Lysenko, H. Krautscheid, E. B. Rusanov, A. N. Chernega, K. W. Kraemer, S. Liu, S. Decurtins and K. V. Domasevitch, *Inorg. Chem.*, 2013, **52**, 863; X. Zhang, J. Zhou, W. Shi, Z. Zhang and P. Cheng, *CrystEngComm*, 2013, **15**, 9738; V. Safarifard and A. Morsali, *CrystEngComm*, 2012, **14**, 5130; S. Saha, G. Das, J. Thote and R. Banerjee, *J. Am. Chem. Soc.*, 2014, **136**, 14845.
 - 7 M. M. Dirtu, C. Neuhausen, A. D. Naik, A. Leonard, F. Robert, J. Marchand-Brynaert, B. Su and Y. Garcia, *Cryst. Growth Des.*, 2011, **11**, 1375; E. Yang, Z. Liu, C. Zhang, Y. Yang and X. Zhao, *Dalton Trans.*, 2013, **42**, 1581; H. Wu, X. Lu, C. Yang, C. Dong and M. Wu, *CrystEngComm*, 2014, **16**, 992; Z. Song, H. Gao, G. Li, Y. Yu, Z. Shi and S. Feng, *CrystEngComm*, 2009, **11**, 1579; Z. Han, R. Lu, Y. Liang, Y. Zhou, Q. Chen and M. Zeng, *Inorg. Chem.*, 2012, **51**, 674; D. Laessig, J. Lincke, J. Moellmer, C. Reichenbach, A. Moeller, R. Glaeser, G. Kalies, K. A. Cychosz, M. Thommes, R. Staudt and H. Krautscheid, *Angew. Chem., Int. Ed.*, 2011, **50**, 10344.
 - 8 P. Yao, H. Liu, F. Huang, F. Feng, X. Qin, M. Huang, Q. Yu and H. Bian, *CrystEngComm*, 2016, **18**, 938; S. Wang, Y. Bi and W. Liao, *CrystEngComm*, 2015, **17**, 2896; A. Tian, Y. Ning, J. Ying, G. Liu, X. Hou, T. Li and X. Wang, *CrystEngComm*, 2015, **17**, 5569; A. Tabacaru, S. Galli, C. Pettinari, N. Masciocchi, T. M. McDonald and J. R. Long, *CrystEngComm*, 2015, **17**, 4992; B. Song, C. Qin, Y. Zhang, X. Wu, H. Liu, K. Shao and Z. Su, *CrystEngComm*, 2015, **17**, 3129; S. Miao, Z. Li, C. Xu and B. Ji, *CrystEngComm*, 2016, **18**, 4636; J. Qin, D. Du, M. Li, X. Lian, L. Dong, M. Bosch, Z. Su, Q. Zhang, S. Li, Y. Lan, S. Yuan and H. Zhou, *J. Am. Chem. Soc.*, 2016, **138**, 5299.
 - 9 X. Gan, M. Chu, J. Yao, W. Geng, X. Zhang, Y. Tian and H. Zhou, *Asian J. Chem.*, 2014, **26**, 257; Y. Yang, F. Jiang, C. Liu, L. Chen, Y. Gai, J. Pang, K. Sui, X. Wan and M. Hong, *Cryst. Growth Des.*, 2016, **16**, 2266; M. Deng, S. Tai, W. Zhang, Y. Wang, J. Zhu, J. Zhang, Y. Ling and Y. Zhou, *CrystEngComm*, 2015, **17**, 6023; Z. Yan, L. Han, Y. Zhao, X. Li, X. Wang, L. Wang and D. Sun, *CrystEngComm*, 2014, **16**, 8747; M. E. Garner, W. Niu, X. Chen, I. Ghiviriga, K. A. Abboud, W. Tan and A. S. Veige, *Dalton Trans.*, 2015, **44**, 1914; C. Zhang, Z. Liu, N. Liu, H. Zhao, E. Yang and X. Zhao, *Dalton Trans.*, 2016, **45**, 11864; B. Stefane, F. Perdih, A. Visnjevac and F. Pozgan, *New J. Chem.*, 2015, **39**, 566; M. Okada, T. Yoden, E. Kawaminami, Y. Shimada, M. Kudoh, Y. Isomura, H. Shikama and T. Fujikura, *Chem. Pharm. Bull.*, 1996, **44**, 1871.
 - 10 W. Minor, M. Cymborowski, Z. Otwinowski and M. Chruszcz, *Acta Crystallogr., Sect. D: Biol. Crystallogr.*, 2006, **62**, 859.

- 11 A. Altomare, M. C. Burla, M. Camalli, G. L. Cascarano, C. Giacovazzo, A. Guagliardi, A. G. G. Moliterni, G. Polidori and R. Spagna, *J. Appl. Crystallogr.*, 1999, **32**, b115–b119; G. M. Sheldrick, *Acta Crystallogr., Sect. A: Found. Crystallogr.*, 2008, **64**, 112.
- 12 A. W. Addison, T. N. Rao, J. Reedijk, J. van Rijn and G. C. Verschoor, *J. Chem. Soc., Dalton Trans.*, 1984, 1349.
- 13 S. I. Vasylevs'kyi, G. A. Senchyk, A. B. Lysenko, E. B. Rusanov, A. N. Chernega, J. Jezierska, H. Krautscheid, K. V. Domasevitch and A. Ozarowski, *Inorg. Chem.*, 2014, **53**, 3642; G. A. Senchyk, A. B. Lysenko, E. B. Rusanov, A. N. Chernega, J. Jezierska, K. V. Domasevitch and A. Ozarowski, *Eur. J. Inorg. Chem.*, 2012, 5802; G. A. Senchyk, A. B. Lysenko, I. Boldog, E. B. Rusanov, A. N. Chernega, H. Krautscheid and K. V. Domasevitch, *Dalton Trans.*, 2012, **41**, 8675; F. L. Liu, L. L. Zhang, R. M. Wang, J. Sun, J. Yang, Z. Chen and D. F. Sun, *CrystEngComm*, 2014, **16**, 2917; X. B. Liu, H. Lin, Z. Y. Xiao, W. D. Fan, A. Huang, R. M. Wang and D. F. Sun, *Dalton Trans.*, 2016, **45**, 3743; Q. G. Meng, X. L. Xin, L. L. Zhang, F. N. Dai, R. M. Wang and D. F. Sun, *J. Mater. Chem. A*, 2015, **3**, 24016–24021; R. M. Wang, X. B. Liu, A. Huang, W. Wang, Z. Y. Xiao, L. L. Zhang and D. F. Sun, *Inorg. Chem.*, 2016, **55**, 1782; R. M. Wang, Q. G. Meng, L. L. Zhang, H. F. Wang, F. N. Dai, W. Y. Guo and D. F. Sun, *Chem. Commun.*, 2014, **50**, 4911.
- 14 G. A. Senchyk, A. B. Lysenko, H. Krautscheid, J. Sieler and K. V. Domasevitch, *Acta Crystallogr., Sect. C: Cryst. Struct. Commun.*, 2008, **64**, m246; A. S. Degtyarenko, M. Handke, K. W. Kramer, S.-X. Liu, S. Decurtins, E. B. Rusanov, L. K. Thompson, H. Krautscheid and K. V. Domasevitch, *Dalton Trans.*, 2014, **43**, 8530; R. M. Wang, Z. Y. Wang, Y. W. Xu, F. N. Dai, L. L. Zhang and D. F. Sun, *Inorg. Chem.*, 2014, **53**, 7086; W. Wang, J. Yang, R. M. Wang, L. L. Zhang, J. F. Yu and D. F. Sun, *Cryst. Growth Des.*, 2015, **15**, 2589; X. Q. Wang, L. L. Zhang, J. Yang, F. L. Liu, F. N. Dai, R. M. Wang and D. F. Sun, *J. Mater. Chem. A*, 2015, **3**, 12777; J. Yang, X. Q. Wang, F. N. Dai, L. L. Zhang, R. M. Wang and D. F. Sun, *Inorg. Chem.*, 2014, **53**, 10649; X. L. Zhao, F. L. Liu, L. L. Zhang, D. Sun, R. M. Wang, Z. F. Ju and D. F. Sun, *Chem. – Eur. J.*, 2014, **20**, 649; Z. F. Zhu, Y. L. Bai, L. L. Zhang, D. F. Sun, J. H. Fang and S. R. Zhu, *Chem. Commun.*, 2014, **50**, 14674.
- 15 R. L. Carlin, *Magnetochemistry*, Springer-Verlag, New York, 1986.
- 16 A. F. Albuquerque, F. Alet, P. Corboz, P. Dayal, A. Feiguin, S. Fuchs, L. Gamper, E. Gull, S. Ürtler, A. Honecker, R. Igarashi, M. Körner, A. Kozhevnikov, A. Läuchli, S. R. Manmana, M. Matsumoto, I. P. McCulloch, F. Michel, R. M. Noack, G. Pawłowski, L. Pollet, T. Pruschke, U. Schollwöck, S. Todo, S. Trebst, M. Troyer, P. Werner and S. Wessel, *J. Magn. Magn. Mater.*, 2007, **310**, 1187.
- 17 Y. L. Bai, V. Tangoulis, R. B. Huang, L. S. Zheng and J. Tao, *Chem. – Eur. J.*, 2009, **15**, 2377.
- 18 A. R. Fortea, P. Alemany, S. Alvarez and E. Ruiz, *Chem. – Eur. J.*, 2001, **7**, 627.
- 19 M. Soler, P. Artus, K. Folting, J. C. Huffman, D. N. Hendrickson and G. Christou, *Inorg. Chem.*, 2001, **40**, 4902.
- 20 J. E. Davies, B. M. Gatehouse and K. S. Murray, *J. Chem. Soc., Chem. Commun.*, 1973, 2523.